Target Location Estimation in Sensor Networks With Quantized Data

Ruixin Niu, *Member, IEEE*, and Pramod K. Varshney, *Fellow, IEEE*

***Abstract*—A signal intensity based maximum-likelihood (ML) target location estimator that uses quantized data is proposed for wireless sensor networks (WSNs). The signal intensity received at local sensors is assumed to be inversely proportional to the square of the distance from the target. The ML estimator and its corresponding Cramér–Rao lower bound (CRLB) are derived. Simulation results show that this estimator is much more accurate than the heuristic weighted average methods, and it can reach the CRLB even with a relatively small amount of data. In addition, the optimal design method for quantization thresholds, as well as two heuristic design methods, are presented. The heuristic design methods, which require minimum prior information about the system, prove to be very robust under various situations.**

***Index Terms*—Cramér–Rao lower bound, location estimation, quantization, wireless sensor networks.**

I. Introduction

With the significant advances in networking, wireless communications, microfabrication, and microprocessors, the topic of wireless sensor networks (WSNs) has become a fast-growing research area. Recently, many aspects of WSNs, including network architectures, routing protocols, distributed data compression and transmission, and distributed signal processing, have drawn extensive attention [1]–[3]. Typically, a WSN consists of a large number of low-cost, low-power, densely distributed, and possibly heterogeneous sensors. Sensor nodes in a WSN are usually battery driven and hence operate on an extremely frugal energy budget, and they have very limited sensing and communication ability.

An important task that WSNs need to perform is target location estimation, which is imperative for an accurate tracking of the target and higher level motion analysis. Many methods for acoustic source localization in sensor networks or sensor arrays are available in the literature [4]–[9]. In [4]–[6], techniques based on direction of arrival (DOA) estimation have been investigated for narrowband sources. For broadband sources, methods based on time-delay of arrival (TDOA) estimation are more suitable [7]–[9]. In a WSN, usually the sensors are very inexpensive and not accurately synchronized, and hence, the TDOA, which requires accurate timing of sensors, is not very practical.

Manuscript received October 22, 2004; revised February 1, 2006. The associate editor coordinating the review of the manuscript and approving it for publication was Dr. Hilde M. Huizenga. This work was presented in part at the 38th Annual Conference on Information Sciences and Systems (CISS'04), Princeton, NJ, March 2004.

The authors are with the Department of Electrical Engineering and Computer Science, Syracuse University, Syracuse, NY 13244 USA (e-mail: rniu@ecs.syr.edu; varshney@ecs.syr.edu).

Digital Object Identifier 10.1109/TSP.2006.882082

In a WSN, typically there are a large number of inexpensive sensors which are densely deployed in a region of interest (ROI). This makes accurate intensity (energy) based target localization possible. Signal intensity measurements are usually used for target detection. Hence, it is very convenient and economical to utilize them to localize a target, without the need for additional sensor functionalities and measurement features, such as the DOA. Energy-based methods have been proposed and developed in [10]–[12]. In [11], least-square methods are proposed to localize a single acoustic source based on the energy ratios between sensors. In [12], a maximum-likelihood (ML) acoustic source localization method has been presented. In both papers, the fact that the intensity (energy) of acoustic signal attenuates as a function of distance from the source, has been used. Energy-based methods are suitable for WSNs because they only require the energy readings of the sensors.

However, in [10]–[12], analog measurements from sensors are required to estimate the source location. For a typical WSN with limited resources (energy and bandwidth), it is important to limit the communication within the network. Therefore, it is desirable that only binary or multibit quantized data be transmitted from local sensors to the processing node (fusion center). Motivated by this, we propose an intensity based ML target location estimation method using only quantized data. In [13], a related work on sensor localization using quantized received signal strength (RSS) is presented. There, quantized pairwise measurements and *a priori* knowledge of reference sensors' locations are employed to estimate sensors' locations. The problem in our work is different from that in [13], because we will estimate a target's location in a sensor field, based on quantized received signal intensity at local sensors and *a priori* information about these sensors' locations.

In the proposed location estimation method, each sensor node collects and processes raw signal from its environment, and then the processed signal is quantized to discrete data. These discrete data are transmitted via a wireless channel to the processing node (fusion center). Based on data transmitted from all N sensor nodes, the processing node estimates the location of the target.

In Section II, we introduce the signal intensity attenuation model and some basic assumptions to formulate the target localization problem. In Section III, the ML estimators that use quantized data and analog data, are developed and their theoretical performance bounds, the Cramér-Rao lower bounds (CRLBs), are derived. Simulation results are provided to show that the ML estimator using quantized data outperforms heuristic weighted average (WA) methods, and that the proposed ML estimator can reach the CRLB even with relatively small amount of data. In

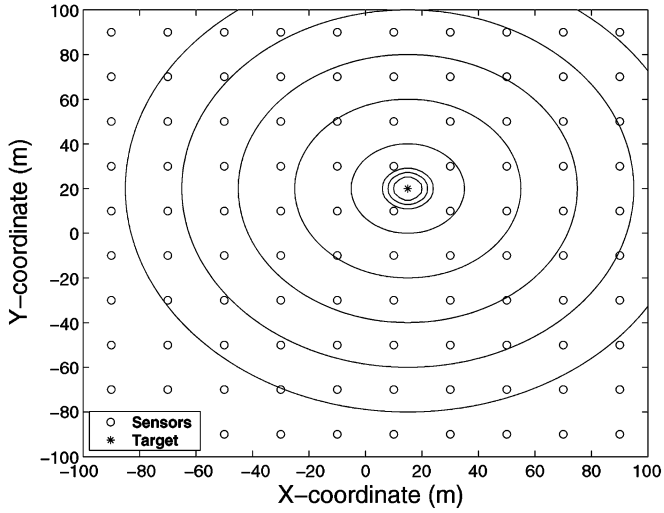

Fig. 1. The signal intensity contours of a target located in a sensor field.

Section IV, the optimal quantization thresholds at local sensors are designed by minimizing the summation of estimation error variances for the target's two coordinates. In Section V, two heuristic quantizer design methods are introduced, which require minimum prior information about the system, and lead to very robust estimation performance under various situations. We present some concluding remarks in Section VI.

II. Problem Formulation

As illustrated in Fig. 1, the signal intensity attenuates as the distance from the target increases. Note that our method can handle any sensor deployment pattern and the uniform sensor deployment shown in Fig. 1 is only a special case. Further, we make the following assumptions:

- A target has been correctly detected in a sensor field with N sensors, whose locations are known.
- We adopt an isotropic signal intensity attenuation model

$$a_i^2 = \frac{G_i P_0'}{\left(\frac{d_i}{d_0}\right)^n} \tag{1}$$

where a_i is the signal amplitude at the ith sensor, G_i is the gain of the ith sensor, P_0' is the emitted power of the target measured at a reference distance d_0, and d_i is the Euclidean distance between the target and the ith sensor

$$d_i = \sqrt{(x_i - x_t)^2 + (y_i - y_t)^2} \tag{2}$$

in which (x_i, y_i) and (x_t, y_t) are the coordinates of the ith sensor and the target, respectively, and n is the power decay exponent. For simplicity, we assume that $G_i = G$ for $i = 1, \cdots, N$, and let $P_0 = GP_0'$. In this paper, we also assume that $d_0 = 1$ m. As a result, (1) becomes

$$a_i^2 = \frac{P_0}{d_i^n}. \tag{3}$$

We assume that all the sensors are in the far field, and the target is at least d_0 meters away from any sensor at all times.

In this paper, we do not specify the type of the passive sensors and the intensity decay model adopted here is quite general. For example, when spherical acoustic waves radiated by a simple source are propagating through the air, the intensity of the waves will decay at a rate inversely proportional to the square of the distance [14]. Similarly, (3) is also a widely adopted model for signal attenuation of an isotropically radiated electromagnetic wave that is propagating in free space [15].

- At each sampling instance, signals emitted from the target are measured by sensors and data collected from all the sensors are called a frame of data. The time interval between frames (samples) is small enough such that the target is assumed static for T frames. As a result, the signal strength at a specific sensor i during frame j, a_{ij}, is invariant for T frames, i.e., $a_{ij} = a_i$ for $j = 1, \cdots, T$.

  This is a reasonable assumption. For example, if the sampling rate is 4000 Hz, a vehicle with a speed of 80 km/h only moves 0.28 m during $T = 50$ sampling intervals.
- At each sensor, the signal a_i is corrupted by an additive Gaussian noise

$$r_{ij} = a_i + \nu_{ij} \tag{4}$$

where r_{ij} is the received signal amplitude at the ith sensor during frame j. The noises follow an identical Gaussian distribution for all the sensors and during all the frames, and they are independent across sensors. To reduce the effect of the additive noise and hence improve the signal-to-noise ratio (SNR), an average received signal amplitude is obtained as follows:

$$\begin{aligned} s_i &\triangleq \frac{1}{T}\sum_{j=1}^{T} r_{ij} \\ &= a_i + \omega_i \end{aligned} \tag{5}$$

where

$$\omega_i \triangleq \frac{1}{T}\sum_{j=1}^{T} \nu_{ij}$$

and obviously it follows a Gaussian distribution. Note that for a sufficiently large T, according to the central limit theorem (CLT), ω_i approaches a Gaussian distribution even for non-Gaussian noises ν_{ij}'s. Here we assume that

$$\omega_i \sim \mathcal{N}(0, \sigma^2)$$

for $i = 1, \cdots, N$. At each sensor, the average signal amplitude s_i is quantized and transmitted to the processing node.

III. Development of Location Estimator Using Quantized Data

A. Location Estimator Using Multibit Data

In this section, we study the location estimation problem using discrete data. We assume that each sensor sends quantized multibit (M-bit) data to the processing node, which are denoted as $\boldsymbol{D} = \{D_i : i = 1, \cdots, N\}$, where D_i can take any discrete value from 0 to $2^M - 1$. To simplify the notation, we define $L = 2^M$. Further, we assume that the set of quantization

thresholds for the ith sensor is $\vec{\eta}_i = [\eta_{i0}, \eta_{i1}, \cdots, \eta_{iL}]$, where $\eta_{i0} = -\infty$ and $\eta_{iL} = \infty$. The quantization process for the ith sensor is such that

$$D_i = \begin{cases} 0 & -\infty < s_i < \eta_{i1} \\ 1 & \eta_{i1} \le s_i < \eta_{i2} \\ \vdots & \vdots \\ L-2 & \eta_{i(L-2)} \le s_i < \eta_{i(L-1)} \\ L-1 & \eta_{i(L-1)} \le s_i < \infty. \end{cases} \tag{6}$$

Due to the Gaussian noise assumption, the probability that D_i takes a specific value l is

$$p_{il}(\vec{\eta}_i, \theta) = Q\left(\frac{\eta_{il} - a_i}{\sigma}\right) - Q\left(\frac{\eta_{i(l+1)} - a_i}{\sigma}\right) \quad (0 \le l \le L-1) \tag{7}$$

where $Q(\cdot)$ is the complementary distribution function of the standard Gaussian distribution

$$Q(x) = \int_x^\infty \frac{1}{\sqrt{2\pi}} e^{-\frac{t^2}{2}} dt. \tag{8}$$

After collecting data $\boldsymbol{D}$, the processing node estimates the parameter vector: $\theta = [P_0 \; x_t \; y_t]'$. Based on the above notations and assumptions listed in Section II, it is easy to derive the likelihood function at the processing node

$$p(\boldsymbol{D}|\theta) = \prod_{i=1}^{N} \prod_{l=0}^{L-1} p_{il}(\vec{\eta}_i, \theta)^{\delta(D_i - l)} \tag{9}$$

where $\delta(\cdot)$ is defined as follows:

$$\delta(x) = \begin{cases} 1, & x = 0 \\ 0, & x \ne 0. \end{cases} \tag{10}$$

The log-likelihood function of $\boldsymbol{D}$ is therefore

$$\ln p(\boldsymbol{D}|\theta) = \sum_{i=1}^{N} \sum_{l=0}^{L-1} \delta(D_i - l) \ln \left[p_{il}(\vec{\eta}_i, \theta)\right]. \tag{11}$$

ML estimation is now the following optimization problem:

$$\max_\theta \ln p(\boldsymbol{D}|\theta). \tag{12}$$

The CRLB for this estimation problem has been derived and stated in the following theorem.

Theorem 1: Assuming the existence of an unbiased estimator $\hat{\theta}(\boldsymbol{D})$, the CRLB is given by

$$E\left\{\left[\hat{\theta}(\boldsymbol{D}) - \theta\right]\left[\hat{\theta}(\boldsymbol{D}) - \theta\right]^T\right\} \ge \boldsymbol{J}^{-1} \tag{13}$$

in which $\boldsymbol{J}$ is the Fisher information matrix (FIM) and its elements are as follows:

$$\begin{aligned} J_{11} &= \sum_i \kappa_i d_i^{-2n}/a_i^2 \\ J_{12} = J_{21} &= n\sum_i \kappa_i d_i^{-(n+2)}(x_i - x_t) \\ J_{13} = J_{31} &= n\sum_i \kappa_i d_i^{-(n+2)}(y_i - y_t) \\ J_{22} &= n^2 \sum_i \kappa_i a_i^2 d_i^{-4}(x_i - x_t)^2 \\ J_{23} = J_{32} &= n^2 \sum_i \kappa_i a_i^2 d_i^{-4}(x_i - x_t)(y_i - y_t) \\ J_{33} &= n^2 \sum_i \kappa_i a_i^2 d_i^{-4}(y_i - y_t)^2 \end{aligned} \tag{14}$$

where

$$\kappa_i = \frac{1}{8\pi\sigma^2} \sum_{l=0}^{L-1} \frac{\gamma_{il}}{p_{il}(\vec{\eta}_i, \theta)}$$

and

$$\gamma_{il} = \left[e^{-\frac{(\eta_{il} - a_i)^2}{2\sigma^2}} - e^{-\frac{\left(\eta_{i(l+1)} - a_i\right)^2}{2\sigma^2}}\right]^2.$$

Proof: See Appendix I.

The closed form of the CRLB matrix $\boldsymbol{R}$ can be derived by taking the inverse of $\boldsymbol{J}$

$$\boldsymbol{R} = \frac{1}{|\boldsymbol{J}|}\begin{bmatrix} J_{22}J_{33} - J_{23}^2 & J_{13}J_{23} - J_{12}J_{33} & J_{12}J_{23} - J_{13}J_{22} \\ J_{13}J_{23} - J_{12}J_{33} & J_{11}J_{33} - J_{13}^2 & J_{12}J_{13} - J_{11}J_{23} \\ J_{12}J_{23} - J_{13}J_{22} & J_{12}J_{13} - J_{11}J_{23} & J_{11}J_{22} - J_{12}^2 \end{bmatrix} \tag{15}$$

where the determinant of $\boldsymbol{J}$ is

$$|\boldsymbol{J}| = J_{11}J_{22}J_{33} + 2J_{12}J_{13}J_{23} - J_{11}J_{23}^2 - J_{22}J_{13}^2 - J_{33}J_{12}^2. \tag{16}$$

B. Location Estimator Using Analog Data

For the purpose of comparison, we have also derived the CRLB of the location estimator using analog data. We denote analog data from N sensors as $\boldsymbol{S} = \{s_i : i = 1, \cdots, N\}$. Based on the additive Gaussian noise assumption, it is easy to show that the log-likelihood function is

$$\ln f(\boldsymbol{S}|\theta) = \sum_{i=1}^{N} \left[-\frac{(s_i - a_i)^2}{2} - \ln\sqrt{2\pi}\right]. \tag{17}$$

The ML estimation procedure is to find the optimal θ that maximizes the log-likelihood

$$\max_\theta \ln f(\boldsymbol{S}|\theta). \tag{18}$$

The FIM for this estimation problem is derived and provided in the following theorem.

Theorem 2: The FIM for estimators using analog data is

$$\boldsymbol{J} = \frac{1}{\sigma^2}\sum_{i=1}^{N}\boldsymbol{C}_i$$

where

$$\boldsymbol{C}_i = \begin{bmatrix} \frac{1}{4P_0 d_i^n} & \frac{n(x_i-x_t)}{4d_i^{n+2}} & \frac{n(y_i-y_t)}{4d_i^{n+2}} \\ \frac{n(x_i-x_t)}{4d_i^{n+2}} & \frac{P_0 n^2(x_i-x_t)^2}{4d_i^{n+4}} & \frac{P_0 n^2(x_i-x_t)(y_i-y_t)}{4d_i^{n+4}} \\ \frac{n(y_i-y_t)}{4d_i^{n+2}} & \frac{P_0 n^2(x_i-x_t)(y_i-y_t)}{4d_i^{n+4}} & \frac{P_0 n^2(y_i-y_t)^2}{4d_i^{n+4}} \end{bmatrix}.$$

Proof: See Appendix II.

The corresponding CRLB matrix $\boldsymbol{R}$ can be derived with a similar procedure as used in Section III-A.

C. Simulation Results

In this subsection, we give simulation results for the ML estimator discussed in Section III-A. For the purpose of comparison, the performances of several heuristic estimation methods based on WAs are also provided.

In order to find the global maximum during ML estimation, we first employ a systematic grid search to find an approximate maximum point. From this point, a sequential quadratic programming (SQP) based procedure provided by MATLAB is used to perform the maximization.

As for the WA methods, the estimated target location is obtained by taking a weighted average of all the sensors' locations. In the first WA method (WA-I), the ith sensor's weight is proportional to the data D_i it sends to the fusion center

$$\hat{\xi}_t = \frac{\sum_{i=1}^{N} D_i \xi_i}{\sum_{i=1}^{N} D_i} \tag{19}$$

where $\xi_t = [x_t\ y_t]'$ and $\xi_i = [x_i\ y_i]'$.

In the second WA method (WA-II), the ith sensor's weight is proportional to the square of the data (D_i) it sends to the fusion center

$$\hat{\xi}_t = \frac{\sum_{i=1}^{N} D_i^2 \xi_i}{\sum_{i=1}^{N} D_i^2}. \tag{20}$$

Note that in both WA-I and WA-II methods, in the case that all the sensors send a "0" to the fusion center, the average (centroid) of all the sensors' location will be taken as the estimate of the target location.

In the third WA method (WA-III), only those sensors, whose data have the highest value of D_i, get equal nonzero weights. Other sensors are assigned a zero weight

$$\hat{\xi}_t = \frac{\sum_{D_i = D_{\max}} \xi_i}{|S_{\max}|} \tag{21}$$

where $D_{\max} = \max_i D_i$, and $|S_{\max}|$ denotes the cardinality of the set $S_{\max} = \{D_i : D_i = D_{\max}, i = 1, \cdots, N\}$. Note that while WA methods can estimate the target's location, they are unable to make an estimate of P_0.

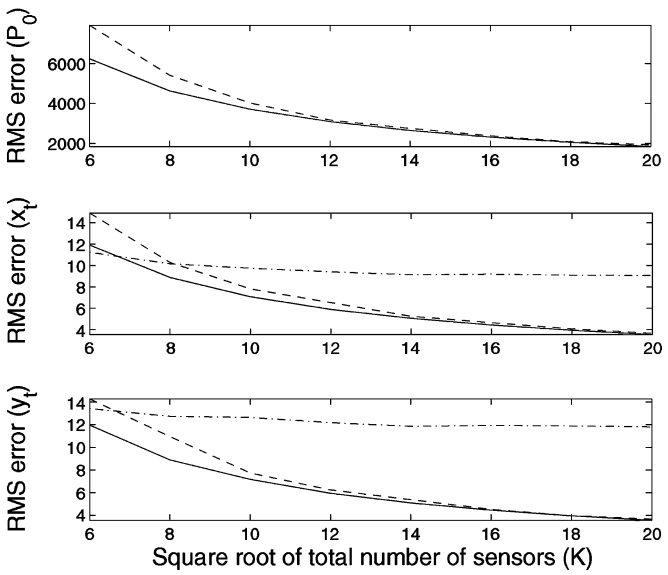

Fig. 2. Root mean square (RMS) errors of different estimation methods ($n = 2, P_0 = 25000, x_t = 15$ m, $y_t = 20$ m, $M = 1, \sigma = 1$). RMS estimation errors for x_t and y_t are in meters. Sensors are uniformly deployed as shown in Fig. 1. Solid line: CRLB, dashed line: ML, dash-dot line: WA. Quantization threshold $\eta = 1.70$.

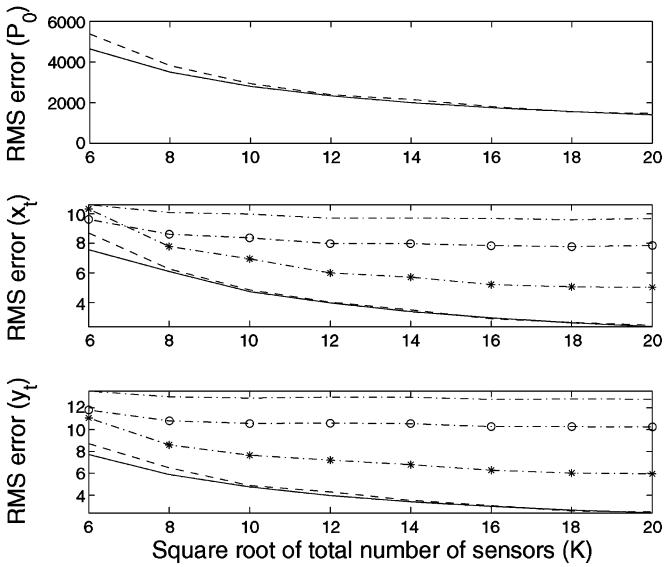

Fig. 3. RMS errors of different estimation methods ($n = 2, P_0 = 25000$, $x_t = 15$ m, $y_t = 20$ m, $M = 2, \sigma = 1$). RMS estimation errors for x_t and y_t are in meters. Sensors are uniformly deployed as shown in Fig. 1. Solid line: CRLB, dashed line: ML, dash-dot line: WA-I, dash-dot line + circle: WA-II, dash-dot line + star: WA-III. Quantization threshold $\vec{\eta} = [0.82, 1.70, 2.72]$.

In Fig. 2, the performance of the ML estimator using binary data is compared with the CRLB and that of the WA methods. The performances are based on 1000 simulation runs. Note that when binary quantization is used by local sensors, all three WA methods are equivalent. Sensors are uniformly deployed as shown in Fig. 1. The performance is plotted as a function of K, where $K = \sqrt{N}$ is the square root of the number of sensors. It is clear that the ML method has a better performance than the WA methods, except when the number of sensors

TABLE I
AVERAGE NEES BASED ON 100 MONTE CARLO RUNS FOR THE ML ESTIMATOR ($n = 2$, $P_0 = 25000$, $x_t = 15$ m, $y_t = 20$ m, $\sigma = 1$)

Total number of sensors (N)	36	64	100	144	196	256	324	400
Binary data ($M = 1$)	4.38	4.17	4.08	3.80	3.35	3.04	3.11	2.85
Quaternary data ($M = 2$)	3.68	3.41	3.20	3.22	2.93	3.18	2.86	3.22

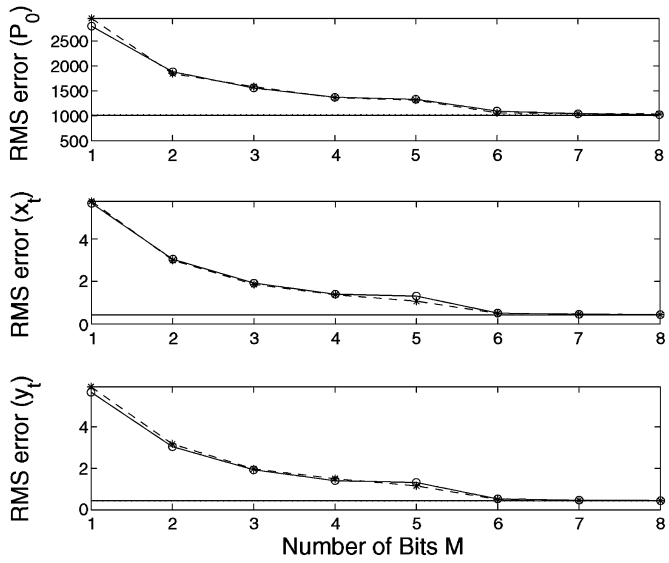

Fig. 4. RMS errors for ML estimators using quantized data and analog data ($n = 2$, $P_0 = 25000$, $x_t = y_t = 0$ m, $N = 196$, $\sigma = 1$). RMS estimation errors for x_t and y_t are in meters. Sensors are uniformly deployed as shown in Fig. 1. Solid line: CRLB for analog data, dotted line: ML estimator using analog data, solid line + circle: CRLB for quantized data, dashed line + star: ML estimator using quantized data. Quantization thresholds are calculated using the Fisher information based heuristic quantization (FIHQ) method, which is described in Section V-B.

in the ROI is relatively small $(N = 36)$. As the number of sensors N increases, the ML estimator's performance improves significantly and quickly converges to the CRLB, but the WA methods do not gain much in estimation accuracy.

In Fig. 3, the performance of the ML estimator using quaternary data is compared with the CRLB and those of heuristic WA methods. It is clear that the ML method has a much better performance than the WA methods. As the number of sensors N increases, the ML estimator's performance quickly converges to the CRLB. Among the WA methods, it appears that in general, the methods that assign a heavier weight to a sensor with a larger quantized data (D_i), achieve a better performance. That is, WA-II and WA-III always outperform WA-I, and WA-III, which only assigns nonzero weights to those sensors with highest D_i's, has the best performance, except when the number of sensors is very small $(N = 36)$. This is not surprising and can be explained intuitively. Because the closer the sensors are to the target, the higher their received signals, and hence the greater quantization outputs they will have. It is better to give those sensors much greater weights than others.

In Fig. 4, the ML estimator using quantized data is compared with that using analog data. Again, the RMS estimation error for the ML estimator is calculated based on 1000 Monte Carlo simulation runs. As we can see, the RMS estimation errors for the ML estimator using analog data is indistinguishable from values obtained from the theoretical CRLB. The performance of the ML estimator using quantized data is also very close to its CRLB. As the number of bits increases, the performance of ML estimator using quantized data converges to that using analog data. The ML estimator based on 6-bit quantized data has little difference from the ML estimator based on analog data, in terms of estimation accuracy.

To verify the results we derived in Section III-A, we use the normalized estimation error squared (NEES) [16], which is defined as

$$\epsilon_\theta = (\theta - \hat{\theta})^T \boldsymbol{J} (\theta - \hat{\theta}) \tag{22}$$

where $\hat{\theta}$ is the estimate, and $\boldsymbol{J}$ is the FIM. It is well known that the ML estimate is asymptotically Gaussian with the mean equal to the true value of the parameter to be estimated and variance given by the CRLB. Assuming that the estimation error is approximately Gaussian, the NEES is Chi-square distributed with n_θ degrees of freedom, where $n_\theta = 3$ is the dimension of the parameter being estimated, namely, θ. For multiple Monte Carlo simulations, the average of NEES is usually used, which is defined as

$$\bar{\epsilon}_\theta = \frac{1}{N_m} \sum_{i=1}^{N_m} \epsilon_\theta^i \tag{23}$$

where N_m is the number of Monte Carlo simulations. $N_m \bar{\epsilon}_\theta$ has a Chi-square density with $N_m n_\theta$ degrees of freedom. Based on 100 Monte Carlo runs, our results are listed in Table I. The two-sided 95% confidence region for the average NEES is $[2.54, 3.50]$. The results show that for a system with binary quantization, when the total number of sensors (N) is greater than or equal to 196, the average NEES falls in the two-sided 95% confidence region. This means that our ML estimator is efficient, that is, the errors "match" the covariance given by the CRLB. For quaternary quantization, the average NEES falls in the 95% confidence region even when the number of sensors is as low as 64.

In Fig. 5, for a WSN with 196 uniformly deployed sensors and binary quantization, the results of location estimation, along with the theoretically calculated covariance are shown. The latter is presented as an ellipse corresponding to the 99% confidence regions of the position estimates based on the CRLB provided by Theorem 1. We can see that in 99 out of 100 Monte Carlo runs, the estimated positions fall in the 99% confidence region.

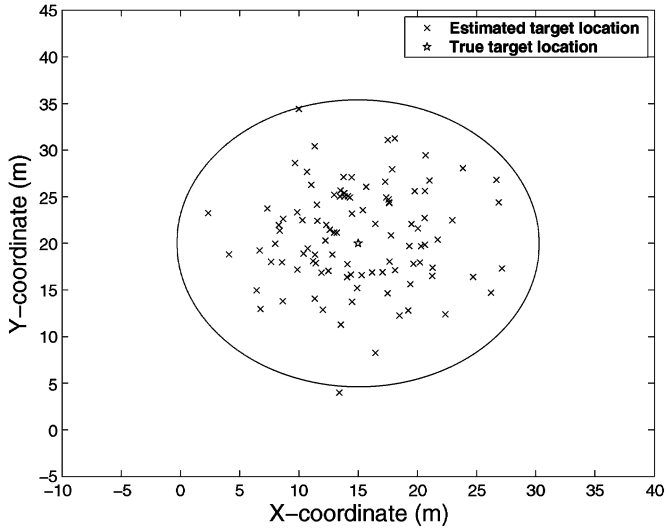

Fig. 5. The true and estimated locations from 100 Monte Carlo runs. Note that in almost all cases the estimated values lie within the respective ellipse. ($n = 2$, $P_0 = 25000$, $x_t = 15$ m, $y_t = 20$ m, $\sigma = 1$, $M = 1$, $N = 196$). Sensors are uniformly deployed as shown in Fig. 1.

IV. Optimal Quantization Thresholds

As we can see from Theorem 1, the FIM and, hence, the CRLB are functions of the quantization thresholds. Therefore, the quantization thresholds at local sensors can be designed to achieve better system performance (estimation accuracy). Because in this paper, we are more concerned about the estimation accuracy of the target location rather than the signal power at distance d_0 (P_0), a natural choice for the cost function is the summation of variances for location estimation errors in two dimensions, namely, the summation of the $(2,2)$ and $(3,3)$ elements of the CRLB matrix. We denote this quantity as V, and from (15), we have

$$V(\vec{\eta}) = \frac{J_{11}(\vec{\eta})\left[J_{33}(\vec{\eta}) + J_{22}(\vec{\eta})\right] - J_{13}^2(\vec{\eta}) - J_{12}^2(\vec{\eta})}{|\boldsymbol{J}(\vec{\eta})|} \quad (24)$$

where $\vec{\eta} = \{\vec{\eta}_i : i = 1, \cdots, N\}$ is the set of thresholds at all the sensors. The optimal threshold set $\vec{\eta}$ is then the solution of the following optimization problem:

$$\min_{\vec{\eta}} V(\vec{\eta}) \quad (25)$$

Note that $\vec{\eta}$ has $N(L-1)$ elements. For example, for a system using 64 sensors and 10-bit quantization, the minimization problem has to be solved over 65 472 variables, and the optimization problem cannot be decoupled into subproblems with smaller number of variables. For simplicity, both in theoretical analysis and in practice, a realistic assumption is that all the sensors employ identical thresholds. The optimization problem can be performed over just $L-1$ variables.

Implicitly, the threshold optimization method proposed in this section requires the knowledge of the signal power P_0, and target location (x_t, y_t), which are nothing but the unknown parameters that need to be estimated. Furthermore, the optimal threshold also depends on the locations of the sensors. For many WSN applications, the sensors will be deployed randomly in a surveillance area. Due to the uncertainty in the locations of these sensors, it is impossible to set the optimal thresholds before deployment. A possible solution is to assume that all the unknown parameters, including P_0, (x_t, y_t), and (x_i, y_i) for $i = 1, \cdots, N$, follow a uniform distribution in an interval (for P_0) and in the surveillance region (for target and sensor locations). An average cost function then can be calculated by employing a multiple-fold integration over these unknown parameters. However, this is a very complicated problem that leads to prohibitive computation load. As a result, the design of optimal threshold is not practical and its corresponding estimation performance can only serve as a benchmark for other quantization thresholds. It is imperative to find some intuitive methods to design quantization thresholds, which should be simple to calculate and robust in various scenarios.

V. Heuristic Methods for Threshold Design

A. Entropy-Based Heuristic Quantization

The entropy-based heuristic quantization (EHQ) method is inspired by the fact that the threshold of a binary quantizer should not be too high or too low, in order to convey useful information about the target. Hence, it is important to investigate the distribution of the signal amplitude a_i. From (2) and (3), we know that the signal amplitude is a function of P_0, (x_i, y_i), and (x_t, y_t). We further assume that the signal power at distance d_0 follows a uniform distribution within the interval $[0, P_m]$

$$f(P_0) = \begin{cases} \frac{1}{P_m}, & 0 < P_0 \le P_m \\ 0, & \text{otherwise} \end{cases} \quad (26)$$

where P_m is the maximum value that P_0 can take. We also assume that x_i, x_t, y_i, y_t are independent and identically distributed (i.i.d.) random variables that follow a uniform distribution in the interval $[-b/2, b/2]$

$$f(x) = \begin{cases} \frac{1}{b}, & -\frac{b}{2} < x \le \frac{b}{2} \\ 0, & \text{otherwise} \end{cases} \quad (27)$$

where b is the length of the ROI, which is a square with area b^2. In addition, the distance between any sensor and the target should be greater than d_0, and the power decay exponent is $n = 2$. Given these assumptions and conditions, we derived the probability density function (pdf) of the signal amplitude measured at a random location, which is stated as follows.

Theorem 3: The pdf of the signal amplitude measured at a random location is

$$f(z) = \frac{2}{\alpha P_m} \begin{cases} \left(\frac{b^2}{3} - \beta\right) z, & 0 < z \le \frac{\sqrt{P_m}}{\sqrt{2}b} \\ \left[\frac{b^2}{15} - \beta + g\left(\frac{P_m}{z^2}\right)\right] z, & \frac{\sqrt{P_m}}{\sqrt{2}b} < z \le \frac{\sqrt{P_m}}{b} \\ \frac{P_m^3}{3b^4 z^5} - \frac{8P_m^{\frac{5}{2}}}{5b^3 z^4} + \frac{\pi P_m^2}{2b^2 z^3} - \beta z, & \frac{\sqrt{P_m}}{b} < z \le \frac{\sqrt{P_m}}{d_0} \\ 0, & \text{o.w.} \end{cases} \quad (28)$$

where

$$\alpha = 1 + \frac{8d_0^3}{3b^3} - \pi\frac{d_0^2}{b^2} - \frac{d_0^4}{2b^4} \quad (29)$$

which is the probability that a sensor is at least d_0 meters away from the target,

$$\beta = \frac{\pi}{2b^2}d_0^4 + \frac{d_0^6}{3b^4} - \frac{8d_0^5}{5b^3} \tag{30}$$

and the function $g(\cdot)$ is defined as

$$g(t) = \frac{t^2}{b^2}arcsin\left(\frac{2b^2}{t} - 1\right) - \frac{t^2}{b^2} - \frac{t^3}{3b^4} + \frac{2}{15b^3}\sqrt{t-b^2}(12t^2 + b^2t + 2b^4). \tag{31}$$

Proof: See Appendix III.

In the theorem, α gives the probability that a sensor is at least d_0 meters away from the target. For $b = 200$ m, the probability that a randomly deployed sensor is within a distance of 1 m from a target with random location, is $1 - \alpha = 7.8 \times 10^{-5}$, which is quite low. Simulations have been carried out to support the theoretical results in Theorem 3. The pdf of the signal amplitude estimated by simulation is identical to that provided by Theorem 3. The simulation results are not shown here due to limited space.

Once the pdf of the signal amplitude $z = a_i$ is available, according to (7), the probability that the quantization process has an output symbol l $(l = 0, \cdots, L-1)$ is

$$P_l = \int_0^{\frac{\sqrt{P_m}}{d_0}} \left[Q\left(\frac{\eta_l - z}{\sigma}\right) - Q\left(\frac{\eta_{(l+1)} - z}{\sigma}\right)\right] f(z)dz. \tag{32}$$

An intuitive method to design quantization thresholds is to maximize the entropy of the symbols sent by sensors. The maximum entropy can be achieved by choosing a set of thresholds so that the probabilities of each symbol are the same, namely $P_l = 1/L$, $(l = 0, \cdots, L-1)$. For example, for a binary quantization, a threshold should be chosen so that both symbols "1" and "0" have a probability of $1/2$. For a WSN with a large number of sensors, there are, on an average, half of the sensors sending "1's" to the processing node and the other half sending "0's." As a result, this method significantly reduces the probability that almost all the sensors are sending the same symbols. The thresholds can be found numerically by using (32).

B. Fisher Information Based Heuristic Quantization (FIHQ)

All the information about $\theta = [P_0\ x_t\ y_t]'$ is contained in sensors' signal amplitudes (a_i's). Intuitively, if all the signal amplitudes a_i $(i = 1, \cdots, N)$ can be accurately recovered from their corresponding quantized data D_i $(i = 1, \cdots, N)$, an accurate estimate of θ can be obtained. Similar to the derivation of (11), the log-likelihood function of quantized data D at any sensor is

$$\ln p(D|z) = \sum_{l=0}^{L-1} \delta(D-l) \ln\left[p_l(\vec{\eta}, z)\right] \tag{33}$$

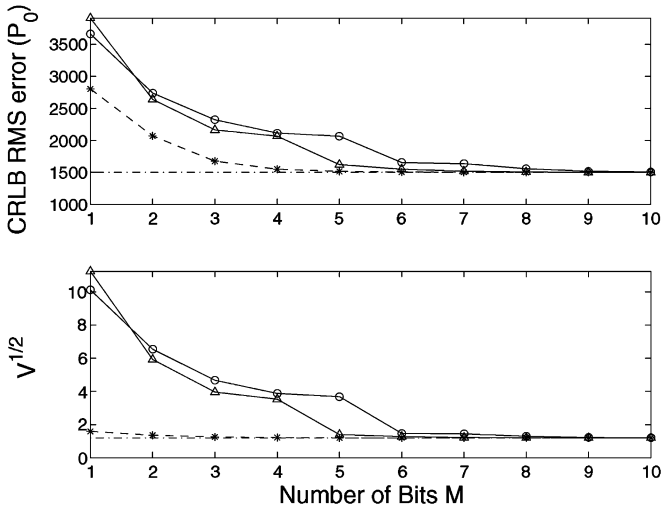

Fig. 6. CRLB RMS errors of estimators using multibit data as a function of number of bits M ($N = 100, n = 2, P_0 = 25000, x_t = y_t = 0$ m, $P_m = 50000, b = 200$ m). Sensors are uniformly deployed as shown in Fig. 1. Dashed line + star: optimal quantization, das-dot line: analog data, solid line + circle: EHQ, solid line + triangle: FIHQ.

where z is the signal amplitude at that sensor. Based on (33), it is not difficult to derive the Fisher information of this scalar estimation problem

$$F(\vec{\eta}) = E\left[\sum_{l=0}^{L-1} \frac{\left[e^{-\frac{(\eta_l - z)^2}{2\sigma^2}} - e^{-\frac{(\eta_{l+1} - z)^2}{2\sigma^2}}\right]^2}{2\pi\sigma^2 p_l(\vec{\eta}, z)}\right] = \int_0^{\frac{\sqrt{P_m}}{d_0}} 4\kappa(\vec{\eta}, z) f(z)dz. \tag{34}$$

Interestingly enough, the Fisher information is proportional to the average value of the scaler κ_i, which has appeared in the FIM provided by Theorem 1. Now its physical meaning is clear. That is, $4\kappa_i$ is nothing but the amount of Fisher information about a_i that is contained in data D_i. The threshold $\vec{\eta}$ then can be designed such that in data D, there is maximum amount of Fisher information about z

$$\max_{\vec{\eta}} F(\vec{\eta}). \tag{35}$$

Since here the Fisher information $F(\vec{\eta})$ is a scalar, maximizing it with respect to $\vec{\eta}$ is equivalent to minimizing its reciprocal, namely the CRLB on the estimation variance.

Note that both of the heuristic methods do not require the knowledge of the sensor location, the target location, or the signal power at distance d_0 (P_0). So the thresholds can be set before deployment, as long as there is some prior knowledge about the ROI (b), and the possible range of P_0, i.e., P_m. These two methods are applicable to situations where sensors are deployed randomly.

C. Performance Evaluation of Heuristic Methods

In Fig. 6, the theoretical values of CRLB on RMS errors are plotted for different quantization methods. For comparison, the CRLB on the estimation RMS errors for the estimator using

TABLE II
SQUARE ROOT OF LOCATION VARIANCE V. ($n = 2$, $P_m = 50000$, $x_t = y_t = 0$ m, $\sigma = 1$, $b = 200$ m, $M = 1$)

P_0	200	1000	4000	10000	20000	40000	50000
Optimal threshold	1.25×10^{12}	1.61×10^{9}	1.47×10^{5}	103.68	2.30	7.87	105.26
EHQ	18.43	8.02	10.17	9.25	9.89	10.93	11.65
FIHQ	17.45	8.47	11.02	10.10	10.94	12.42	13.40

analog data is also plotted. In this figure, V is the summation of the variances for estimation errors of x_t and y_t, as defined in (24).

As we can see, the optimal thresholds provide a significant improvement in estimation accuracy, compared with those given by EHQ and FIHQ. As the number of bits M increases, the CRLB on RMS error for multibit data converges to that for analog data, for all the three quantization methods. The superiority of the optimal thresholds is not surprising, because much more knowledge, including the sensors' locations, the target's location, and the exact value of P_0 has been used. Another phenomenon is that when binary data are used, EHQ outperforms FIHQ; when multibit data are employed, FIHQ has a better performance. This is because the main intuition behind EHQ is to improve robustness, as explained in Section V-A. When binary data are used, robustness is a critical issue and EHQ outperforms FIHQ. However, there is no explicit and direct relationship between the entropy of symbols and estimation performance, especially when $M > 1$. On the other hand, for FIHQ, the physical meaning of Fisher information is well understood, and we know heuristically that larger Fisher information usually leads to a better estimation performance, as explained in Section V-B. Hence, it is not surprising that based on multibit data, FIHQ has a better performance than EHQ.

It is important to test the performance of all the three kinds of quantization thresholds for various system parameters. We assume that the optimal thresholds, which are obtained by using the parameters given in Fig. 6, remain the same in all the examples below.

First, the target location is changed to $(5, 10)$ instead of $(0, 0)$. The results are shown in Fig. 7. As we can see, when binary quantization is used, the MSE errors for optimal thresholds are much higher than heuristic methods. To make things even worse, even when the number of bits is very large $(M = 10)$, the performance for optimal thresholds cannot reach that of analog data. On the contrary, both of the two heuristic methods provide reliable performances.

Based on the above example, an important observation is that the choice of thresholds is critical when binary quantization is used. Now we keep the target location as $(0, 0)$, and introduce a mismatch in P_0. In Table II, the performances of the estimator using "mismatched" optimal threshold, and those using heuristic thresholds are listed for varying P_0s. Again, the optimal threshold gives a very poor performance for "mismatched" P_0 values. For example, when $P_0 = 200$, the optimal threshold leads to an ill-conditioned estimation problem and gives rise to an estimation error of $\sqrt{V} = 1.25 \times 10^{12}$ meters. This is because the optimal thresholds, which are designed to match a greater P_0, are too high in this case. There are hardly any "1"s that are sent to the processing node. By contrast, both the EHQ and FIHQ methods, which require minimum prior information about the system, have very robust performances, even when P_0 has extreme values.

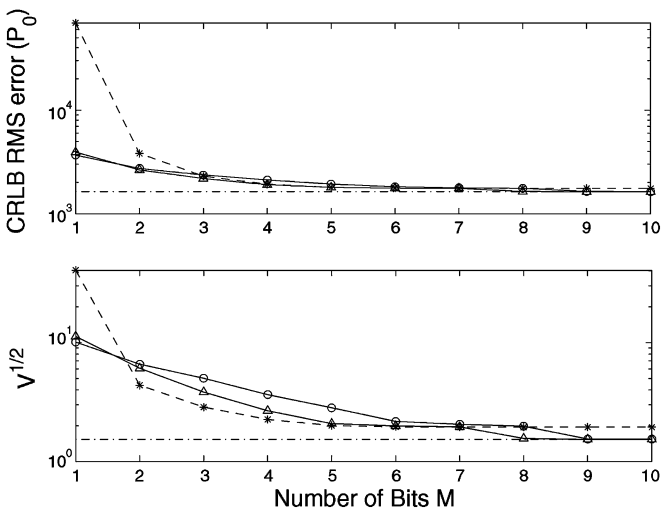

Fig. 7. CRLB RMS errors of estimators using multibit data as a function of number of bits M ($N = 100$, $n = 2$, $P_0 = 25000$, $x_t = 5$ m, $y_t = 10$ m, $P_m = 50000$, $b = 200$ m). Sensors are uniformly deployed as shown in Fig. 1. Dashed line + star: optimal thresholds, dash-dot line: analog data, solid line + circle: EHQ, solid line + triangle: FIHQ.

VI. CONCLUSION AND DISCUSSION

In this paper, based on an isotropic signal attenuation model, we presented an intensity-based ML target location estimator that uses quantized data for WSNs. Simulation results show that this estimator is much more accurate than heuristic weighted average methods and it is efficient even with a very small number of quantization bits and a relatively small number of sensors. In addition, the estimator's corresponding CRLB is derived. Its performance bound (CRLB) converges to that of the estimator using analog data very quickly as the number of bits M increases. The optimal quantization thresholds at local sensors are designed to obtain a better estimation performance. In addition, more practical and heuristic quantizer design methods are presented and are shown to be very robust under various situations.

In this paper, the effect of small-scale fading due to multipath is not considered. In many practical situations, the assumption that the source is omnidirectional and the propagation of the signal is isotropic may not be true. Our future work will include research on target localization under these imperfect situations. Also, our algorithm proposed here deals with a single target, and it can be modified and extended to deal with multiple targets in the future.

APPENDIX I
PROOF OF THEOREM 1

As we know, the FIM can be obtained as follows:

$$\boldsymbol{J} = -E\left[\nabla_\theta \nabla_\theta^T \ln p(\boldsymbol{D}|\theta)\right]. \tag{36}$$

First, we derive the (1,1) element of $\boldsymbol{J}$. From (11), we have

$$\frac{\partial^2 \ln p(\boldsymbol{D}|\theta)}{\partial P_0^2} = \sum_i \sum_l -\frac{\delta(D_i - l)}{p_{il}^2(\vec{\eta}_i,\theta)}\left[\frac{\partial p_{il}(\vec{\eta}_i,\theta)}{\partial P_0}\right]^2 + \frac{\delta(D_i - l)}{p_{il}(\vec{\eta}_i,\theta)}\frac{\partial^2 p_{il}(\vec{\eta}_i,\theta)}{\partial P_0^2} \tag{37}$$

and

$$E\left[\frac{\partial^2 \ln p(\boldsymbol{D}|\theta)}{\partial P_0^2}\right] = \sum_i \sum_l \frac{-1}{p_{il}}\left[\frac{\partial p_{il}}{\partial P_0}\right]^2. \tag{38}$$

Note the fact that $E[\delta(D_i - l)] = p_{il}(\vec{\eta}_i,\theta)$ has been used in the derivation of (38). With

$$\frac{\partial Q\left[(\eta_{il} - a_i)/\sigma\right]}{\partial P_0} = \frac{e^{-\frac{(\eta_{il}-a_i)^2}{2\sigma^2}}}{2\sqrt{2\pi}\sigma a_i d_i^n} \tag{39}$$

it is easy to show that

$$\left[\frac{\partial p_{il}(\vec{\eta}_i,\theta)}{\partial P_0}\right]^2 = \frac{\gamma_{il}}{8\pi\sigma^2 a_i^2 d_i^{2n}}. \tag{40}$$

Substituting (40) into (38), we finally have

$$E\left[\frac{\partial^2 \ln p(D|\theta)}{\partial P_0^2}\right] = \sum_{i=1}^N -\frac{\kappa_i}{a_i^2 d_i^{2n}}. \tag{41}$$

Following a similar procedure, it is easy to derive other elements of $\boldsymbol{J}$. We skip their derivations for the sake of brevity of the paper.

APPENDIX II
PROOF OF THEOREM 2

First, we derive the $(1,1)$ element of $\boldsymbol{J}$. From (17), we have

$$\frac{\partial^2 \ln f(\boldsymbol{S}|\theta)}{\partial P_0^2} = \frac{1}{\sigma^2}\sum_{i=1}^N (s_i - a_i)\frac{\partial^2 a_i}{\partial P_0^2} - \left(\frac{\partial a_i}{\partial P_0}\right)^2. \tag{42}$$

Therefore

$$E\left[\frac{\partial^2 \ln f(\boldsymbol{S}|\theta)}{\partial P_0^2}\right] = \frac{1}{\sigma^2}\sum_{i=1}^N -\left(\frac{\partial a_i}{\partial P_0}\right)^2 \tag{43}$$

where the fact that $E[s_i] = a_i$ has been used. With

$$\frac{\partial a_i}{\partial P_0} = \frac{1}{2\sqrt{P_0 d_i^n}} \tag{44}$$

it is easy to show that

$$E\left[\frac{\partial^2 \ln f(\boldsymbol{S}|\theta)}{\partial P_0^2}\right] = \frac{1}{\sigma^2}\sum_{i=1}^N \frac{-1}{4P_0 d_i^n}. \tag{45}$$

Similarly, it is easy to derive other elements of $\boldsymbol{J}$. We skip their derivations for the sake of brevity of the paper.

APPENDIX III
PROOF OF THEOREM 3

We have assumed that x_i and $-x_t$ are i.i.d. and follow a uniform distribution in the interval $[-b/2, b/2]$. Define $t = x_i - x_t$. The pdf of t equals the convolution of the two uniform pdf functions

$$f_T(t) = \begin{cases} \frac{b+t}{b^2}, & -b < t \le 0 \\ \frac{b-t}{b^2}, & 0 < t \le b \\ 0, & \text{otherwise.} \end{cases} \tag{46}$$

Given the pdf of t, it is easy to show that u, which is defined as $u \triangleq (x_i - x_t)^2 = t^2$, has the following pdf:

$$f_U(u) = \begin{cases} \frac{1}{b\sqrt{u}} - \frac{1}{b^2}, & 0 < u \le b^2 \\ 0, & \text{otherwise.} \end{cases} \tag{47}$$

Define $v = (x_i - x_t)^2 + (y_i - y_t)^2$ as the square of the distance from a sensor to the target. Obviously, the pdf of v is the convolution of two $f_U(\cdot)$ functions

$$f_V(v) = \begin{cases} \frac{\pi}{b^2} + \frac{v}{b^4} - \frac{4\sqrt{v}}{b^3}, & 0 < v \le b^2 \\ \frac{2}{b^2}\arcsin\left(\frac{2b^2 - v}{v}\right) - \frac{v}{b^4} & \\ \quad + \frac{4\sqrt{v - b^2}}{b^3} - \frac{2}{b^2}, & b^2 < v \le 2b^2 \\ 0, & \text{otherwise.} \end{cases} \tag{48}$$

The probability of a sensor is at least d_0 meters away from the target is therefore

$$\begin{aligned} \alpha &= 1 - \int_0^{d_0^2}\left(\frac{\pi}{b^2} + \frac{v}{b^4} - \frac{4\sqrt{v}}{b^3}\right)dv \\ &= 1 + \frac{8d_0^3}{3b^3} - \frac{\pi d_0^2}{b^2} - \frac{d_0^4}{2b^4}. \end{aligned} \tag{49}$$

Hence, given the condition $v \ge d_0^2$, the pdf of v is

$$f_V\left(v|v \ge d_0^2\right) = \frac{1}{\alpha} f_V(v) \quad \left(d_0^2 \le v \le 2b^2\right). \tag{50}$$

In this paper, we choose $n = 2$, and define that $w = a_i^2$. Therefore, $w = P_0/v$. We also assume that P_0 follows a uniform distribution in $[0, P_m]$. Because P_0 and v are independent, we have

$$f_W(w) = \int_{d_0^2}^{2b^2} v f_P(wv) f_v\left(v|v \ge d_0^2\right) dv \tag{51}$$

where $f_P(\cdot)$ denotes the pdf of P_0. Here we skip the tedious derivation and give the results as follows:

$$f_W(w) = \frac{1}{\alpha P_m} \begin{cases} \frac{b^2}{3} - \beta, & 0 < w \le \frac{P_m}{2b^2} \\ \frac{b^2}{15} - \beta + g(s), & \frac{P_m}{2b^2} < w \le \frac{P_m}{b^2} \\ \frac{s^3}{3b^4} - \frac{8s^{\frac{5}{2}}}{5b^3} + \frac{\pi s^2}{2b^2} - \beta, & \frac{P_m}{b^2} < w < \frac{P_m}{d_0^2} \\ 0, & \text{otherwise} \end{cases} \tag{52}$$

where $s = P_m/w$, and function $g(\cdot)$ has been defined in Theorem 3. Finally, we define $z = \sqrt{w}$ and its pdf can be easily derived through the following relationship:

$$f_Z(z) = 2z f_W(z^2). \tag{53}$$

ACKNOWLEDGMENT

The authors are very grateful for the valuable comments and suggestions made by the reviewers.

REFERENCES

[1] S. Kumar, F. Zhao, and D. Shepherd, Eds., "Special issue on collaborative signal and information processing in microsensor networks," *IEEE Signal Process. Mag.*, vol. 19, no. 2, Mar. 2002.

[2] H. Gharavi and S. Kumar, Eds., "Special issue on sensor networks and applications," *Proc. IEEE*, vol. 91, no. 8, pp. 1151–1256, Aug. 2003.

[3] A. Sayeed, D. Estrin, G. Pottie, and K. Ramchandran, Eds., "Special issue on self-organizing distributed collaborative sensor networks," *IEEE J. Sel. Areas Commun.*, vol. 23, no. 4, pp. 689–872, Apr. 2005.

[4] Y. Oshman and P. Davidson, "Optimization of observer trajectories for bearings-only target localization," *IEEE Trans. Aerosp. Electron. Syst.*, vol. 35, no. 3, pp. 892–902, Jul. 1999.

[5] L. M. Kaplan, Q. Le, and P. Molnar, "Maximum likelihood methods for bearings-only target localization," in *Proc. Int. Conf. Acoustics, Speech, and Signal Processing (ICASSP2001)*, Salt Lake City, UT, May 2001, vol. 5, pp. 3001–3004.

[6] S. Haykin, *Array Signal Processing*. Englewood Cliffs, NJ: Prentice-Hall, 1984.

[7] K. Yao, R. E. Hudson, C. W. Reed, D. Chen, and F. Lorenzelli, "Blind beamforming on a randomly distributed sensor array system," *IEEE J. Sel. Areas Commun.*, vol. 16, no. 8, pp. 1555–1567, Oct. 1998.

[8] C. W. Reed, R. E. Hudson, and K. Yao, "Direct joint source localization and propagation speed estimation," in *Proc. Int. Conf. Acoustics, Speech, and Signal Processing (ICASSP99)*, Phoenix, AZ, Mar. 1999, vol. 3, pp. 1169–1172.

[9] J. C. Chen, R. E. Hudson, and K. Yao, "A maximum likelihood parametric approach to source localization," in *Proc. Int. Conf. Acoustics, Speech, and Signal Processing (ICASSP2001)*, Salt Lake City, UT, May 2001, vol. 5, pp. 3013–3016.

[10] D. Li, K. D. Wong, Y. H. Hu, and A. M. Sayeed, "Detection, classification, and tracking of targets," *IEEE Signal Process. Mag.*, vol. 19, no. 3, pp. 17–29, Mar. 2002.

[11] D. Li and Y. H. Hu, "Energy based collaborative source localization using acoustic microsensor array," *EURASIP J. Appl. Signal Process.*, no. 4, pp. 321–337, 2003.

[12] X. Sheng and Y. H. Hu, "Maximum likelihood multiple-source localization using acoustic energy measurements with wireless sensor networks," *IEEE Trans. Signal Process.*, vol. 53, no. 1, pp. 44–53, Jan. 2005.

[13] N. Patwari and A. O. Hero, "Using proximity and quantized RSS for sensor localization in wireless networks," in *Proc. 2nd Int. ACM Workshop on Wireless Sensor Networks and Applications*, San Diego, CA, Sep. 2003, pp. 20–29.

[14] L. E. Kinsler and A. R. Frey, *Fundamentals of Acoustics*. New York: Wiley, 1962.

[15] N. Levanon, *Radar Principles*. New York: Wiley, 1988.

[16] Y. Bar-Shalom and X. R. Li, *Estimation and Tracking—Principles, Techniques, and Software*. Boston, MA: Artech House, 1993.

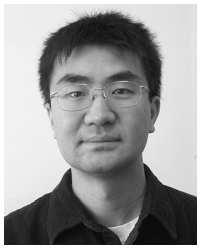

Ruixin Niu (M'04) received the B.S. degree from Xi'an Jiaotong University, Xi'an, China, in 1994, the M.S. degree from the Institute of Electronics, Chinese Academy of Sciences, Beijing, in 1997, and the Ph.D. degree from the University of Connecticut, Storrs, in 2001, all in electrical engineering.

He is currently a Research Assistant Professor with Syracuse University, Syracuse, NY. His research interests are in the areas of statistical signal processing and its applications, including detection, estimation, data fusion, communications, and image processing.

Dr. Niu received the Fusion 2004 Best Paper Award, at the Seventh International Conference on Information Fusion, Stockholm, Sweden, in June 2004.

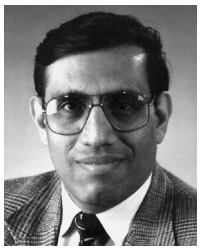

Pramod K. Varshney (F'97) was born in Allahabad, India, on July 1, 1952. He received the B.S. degree in electrical engineering and computer science (with highest honors), and the M.S. and Ph.D. degrees in electrical engineering from the University of Illinois at Urbana-Champaign in 1972, 1974, and 1976 respectively.

From 1972 to 1976, he held teaching and research assistantships at the University of Illinois. While there, he was a James Scholar, a Bronze Tablet Senior, and a Fellow. Since 1976, he has been with the Electrical and Computer Engineering Department, Syracuse University, Syracuse, NY, where he is currently a Professor of Electrical Engineering and Computer Science. He served as the Associate Chairman of the Department from 1993 to 1996. At present, he is the Research Director of The New York State Center for Advanced Technology in Computer Applications and Software Engineering (CASE). His current research interests are in distributed sensor networks and data fusion, detection and estimation theory, wireless communications, image processing, radar signal processing, and parallel algorithms. He has supervised 25 Ph.D. dissertations and authored or coauthored over 70 journal papers and over 170 conference papers. He is the author of *Distributed Detection and Data Fusion* (New York: Springer-Verlag, 1997). He has consulted for General Electric, Hughes, Booz-Allen and Hamilton, Kaman Sciences Corporation, SCEEE, Andro Consulting, and Digicomp Research.

Dr. Varshney is on the editorial boards of *Cluster Computing and Information Fusion*. He is a member of Tau Beta Pi and is the recipient of the 1981 ASEE Dow Outstanding Young Faculty Award. In 2000, he received the Third Millennium Medal from the IEEE and Chancellor's Citation for Exceptional Academic Achievement at Syracuse University. He was the Guest Editor of the Special Issue on Data Fusion of the PROCEEDINGS OF THE IEEE in January 1997. He is a Distinguished Lecturer for the IEEE AES Society. He was the President of the International Society of Information Fusion.